AXAF alignment test system autocollimating flat error correction

Timothy S. Lewis

Eastman Kodak Company
Rochester, NY 14653-5305

ABSTRACT

The alignment test system for the AXAF high-resolution mirror assembly (HRMA) determines the misalignment of the HRMA by measuring the displacement of a beam of light reflected by the HRMA mirrors and an autocollimating flat (ACF). This report shows how to calibrate the system to compensate for errors introduced by the ACF, using measurements taken with the ACF in different positions. It also shows what information can be obtained from alignment test data regarding errors in the shapes of the HRMA mirrors. Simulated results based on measured ACF surface data are presented.

1 INTRODUCTION

The AXAF high-resolution mirror assembly (HRMA) consists of concentric pairs of grazing-incidence paraboloidal and hyperboloidal mirrors, as shown in Figure 1. X-rays entering the telescope parallel to the z axis are first deflected by the paraboloid towards its focus, which coincides with the far focus of the hyperboloid, and then deflected by the hyperboloid to its near focus, which is the system focus. During assembly, the paraboloid is first aligned to the far focus, and then the hyperboloid is added and aligned to the system focus with the paraboloid in place. The alignment test system consists basically of a light source and detector located at the appropriate focus, and a flat mirror (the autocollimating flat, or ACF) located below the HRMA normal to the optical axis. When the HRMA mirrors are perfectly aligned, a beam of light emitted from the focus will emerge from the HRMA parallel to the optical axis, bounce off the ACF, and return to the focus. If the mirrors are misaligned, the beam will be displaced when it returns to the focal plane. Measurements of beam displacements at a number of points around the HRMA can be used to determine the type and amount of misalignment, which can then be corrected. The measurements can also provide some information about errors in the shapes of the HRMA mirrors.

If the surface of the ACF is not perfectly flat, it too can cause displacements of the beam. These displacements can be distinguished from those caused by HRMA misalignment by taking measurements with the ACF in different positions: beam displacements caused by the HRMA should remain constant when the ACF is moved, while those caused by the ACF should change in a predictable way. This report shows how to use these measurements to calibrate the system to compensate for ACF errors. More details are given in an earlier report.[1]

Section 2 shows how beam displacements are related to arbitrary errors in any of the mirrors, and shows how HRMA misalignment errors and certain HRMA shape errors can be determined from the Fourier coefficients of

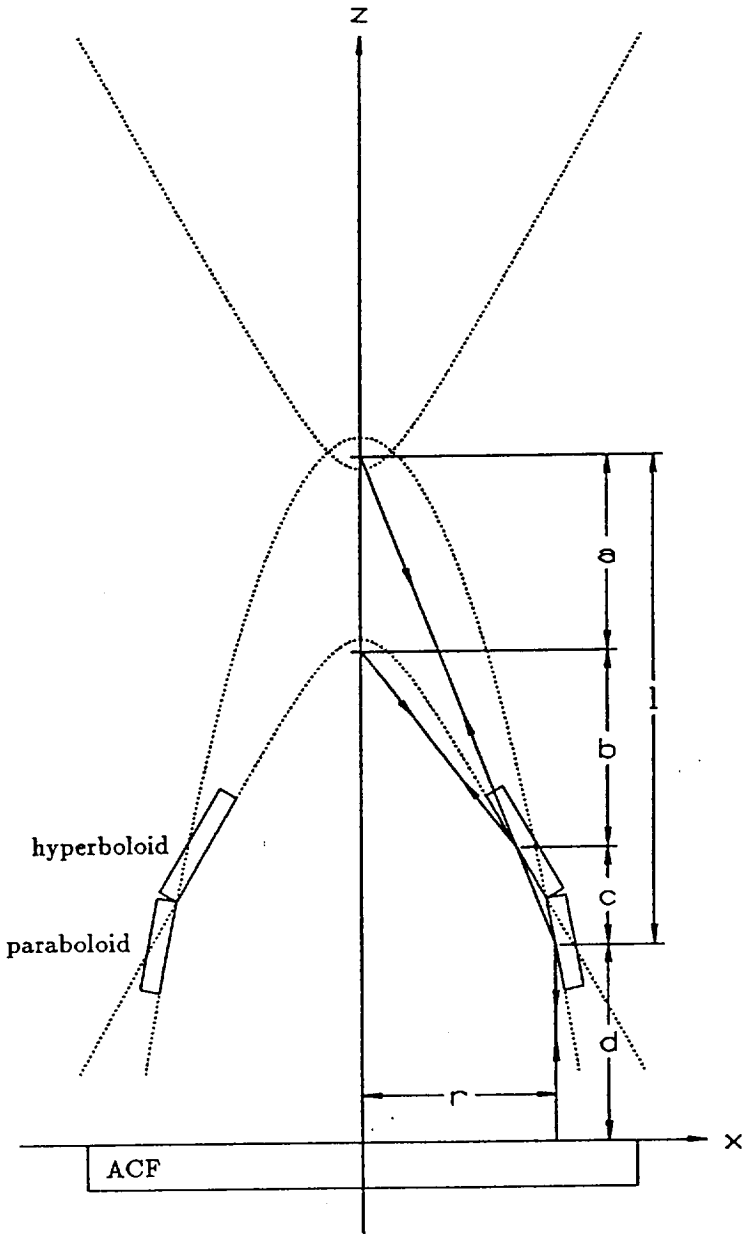

Figure 1: Paraboloidal and hyperboloidal HRMA mirrors with rays from foci to ACF and back, assuming all mirrors are perfect and perfectly aligned.

the beam displacements. Section 3 discusses the effect of ACF errors and shows how to calculate calibration coefficients to compensate for them. Section 4 presents some simulated results based on measured ACF surface data, and Section 5 shows how small random tilts occurring when the ACF is moved will affect the alignment procedure.

2 HRMA ERRORS

We use the coordinate system xyz shown in Figure 1, and define polar coordinates r and θ by $x + iy = re^{i\theta}$. The equations of the paraboloid and hyperboloid are $r^2 = p^2 + 2p(a+\zeta)$ and $r^2 = e^2(h+\zeta)^2 - \zeta^2$, respectively,[2] where ζ is distance from the system focus along the $-z$ axis, a is the distance between the hyperboloid foci, p and h are given constants, and $e = (1 - 2h/a)^{-1/2}$. In practice $a = 10069\,\text{mm}$ for all the mirror pairs, $p = 8.933\,\text{mm}$ and $h = 8.945\,\text{mm}$ for the outermost mirror pair, and $p = 2.496\,\text{mm}$ and $h = 2.497\,\text{mm}$ for the innermost mirror pair. The hyperboloids extend from $\zeta = 9180$ to $10018\,\text{mm}$, and the paraboloids from $\zeta = 10099$ to $10937\,\text{mm}$. Coordinate ζ is given by $\zeta = b + c + d - z$, where b, c, and d are defined in Figure 1. In practice $b \approx a \approx 10\,\text{m}$, $c \approx 900\,\text{mm}$, and $d \approx 2\,\text{m}$. We also define $l = a + b + c$.

Let $\delta(r,\theta) = \Delta x + i\Delta y$ be the displacement in the focal plane of the ray that hits the ACF at point $re^{i\theta}$. In practice we actually measure the average displacement of a beam of rays passing through a small circular aperture above the ACF centered at the point $re^{i\theta}$. There are 24 apertures spaced uniformly in θ at the mean radius r of each paraboloid. The size of each aperture is such as to illuminate two-thirds of the lengths of the HRMA mirrors.

The relationship between the beam displacement δ and the errors in the mirrors can be found by ray tracing. Suppose the surfaces of the paraboloid, hyperboloid, and ACF are given by

$$r = \sqrt{p^2 + 2p(a+\zeta)} - \psi(z,\theta), \quad r = \sqrt{e^2(h+\zeta)^2 - \zeta^2} - \eta(z,\theta), \quad \text{and} \quad z = f(x,y), \tag{1}$$

respectively, where ψ, η, and f represent arbitrary errors, which are assumed to be small enough that only terms linear in ψ, η, f, and their derivatives need be retained in the analysis. For the case of a paraboloid alone, if we trace a ray from the far focus to the ACF and back we find, after no small amount of work, that the displacement of the ray on its return to the focal plane is

$$\delta = -2\left(\psi + i\frac{\partial\psi}{\partial\theta} + 2l\frac{\partial\psi}{\partial z}\right)e^{i\theta} + 2l\left(\frac{\partial f}{\partial x} - i\frac{\partial f}{\partial y}\right)e^{2i\theta}. \tag{2}$$

For the case of the paraboloid and hyperboloid together, if we trace a ray from the system focus to the ACF and back we find, after an even less small amount of work, that the displacement of the ray is

$$\delta = \left(\psi - i\frac{\partial\psi}{\partial\theta} + 4a\frac{\partial\psi}{\partial z} - 3\eta - i\frac{\partial\eta}{\partial\theta} - 4a\frac{\partial\eta}{\partial z}\right)e^{i\theta} - 2a\left(\frac{\partial f}{\partial x} + i\frac{\partial f}{\partial y}\right). \tag{3}$$

The beam displacements were derived exactly in closed form using a computer algebra system, but (2) and (3) have been simplified from the exact final results using $p << l$, $p << a$, $h << a$, $p \approx h$, and $b \approx a$.

Suppose the paraboloid is moved so that its focus is displaced by a small amount (x_p, y_p, z_p) from its correct position, and its axis is tilted in some direction β_p to make a small angle α_p with the z axis, so that the unit vector along the mirror axis pointing out of the telescope is $(\alpha_p \cos\beta_p, \alpha_p \sin\beta_p, -1)$. If these are the only errors present then it can be shown using (2) that the beam displacement will be

$$\delta = 2(x_p + iy_p) + \frac{2r}{l}z_p e^{i\theta} - 2l\alpha_p e^{-i\beta_p}e^{2i\theta}. \tag{4}$$

If we define similar misalignment parameters x_h, y_h, z_h, α_h, and β_h for the hyperboloid, then for a paraboloid

and hyperboloid together the beam displacement will be

$$\delta = 2(x_h + iy_h) + 2a\alpha_p e^{i\beta_p} + \frac{r}{2a}(5z_h - z_p)e^{i\theta} + \left[(x_h - iy_h) - (x_p - iy_p) - a\alpha_h e^{-i\beta_h}\right] e^{2i\theta}. \tag{5}$$

Thus we see that misalignment of the HRMA mirrors causes beam displacements of the form $\delta = q_0 + q_1 e^{i\theta} + q_2 e^{2i\theta}$.

To determine q_0, q_1, and q_2 we measure $\delta(\theta)$ at N points $\theta_j = \theta_0 + 2\pi j/N$, $j = 0, 1, \ldots, N-1$, and then calculate the modified Fourier transform

$$\phi_k = \frac{1}{N}\sum_{j=0}^{N-1} \delta(\theta_j) e^{-ik\theta_j}, \qquad k = 0, 1, \ldots, N-1. \tag{6}$$

This is related to the usual Fourier transform ψ_k of $\delta(\theta_j)$ by $\phi_k = e^{-ik\theta_0}\psi_k$. In practice the aperture plate has $\theta_0 = \pi/N$ and $N = 24$. Any function $\delta(\theta)$ can be represented by an infinite Fourier series

$$\delta(\theta) = \sum_{k=-\infty}^{\infty} q_k e^{ik\theta}. \tag{7}$$

Applying (6) to (7) gives $\phi_k = \hat{q}_k$, where the symbol $\hat{}$ on a quantity indicates that it includes aliased terms:

$$\hat{q}_k = \sum_{j=-\infty}^{\infty} q_{k+jN} e^{ijN\theta_0}. \tag{8}$$

Thus in practice we cannot calculate the desired coefficients q_0, q_1, and q_2, but only $\hat{q}_0$, $\hat{q}_1$, and $\hat{q}_2$, which contain aliased terms. Coefficient $\hat{q}_0$, for example, includes not only the axisymmetric term q_0, but also q_N, q_{2N}, etc., which appear axisymmetric when sampled at N points. If we assume these higher order terms are small then $\hat{q}_0$, $\hat{q}_1$, and $\hat{q}_2$ should be close to q_0, q_1, and q_2.

In addition to $\hat{q}_0$, $\hat{q}_1$, and $\hat{q}_2$, we can also calculate $\hat{q}_3$, $\hat{q}_4$, $\ldots \hat{q}_{N-1}$, which may contain some useful information about errors in the shapes of the HRMA mirrors. Note that coefficients $\hat{q}_{N-1}$, $\hat{q}_{N-2}$, $\ldots$ are directly related to coefficients $\hat{q}_{-1}$, $\hat{q}_{-2}$, $\ldots$. In particular, for any k we have

$$\hat{q}_{k+N} = e^{-iN\theta_0}\hat{q}_k \quad \text{and} \quad \hat{q}_{-k} = e^{iN\theta_0}\hat{q}_{N-k}. \tag{9}$$

If $\theta_0 = \pi/N$ then $\hat{q}_{-k} = -\hat{q}_{N-k}$. Following Glenn,[3] we expand the HRMA error functions ψ and η in the Fourier-Legendre series

$$\psi(z,\theta) = \sum_{n=0}^{\infty}\sum_{m=-\infty}^{\infty} \psi_{nm} P_n\left(\frac{d-z}{w}\right) e^{im\theta}, \quad \eta(z,\theta) = \sum_{n=0}^{\infty}\sum_{m=-\infty}^{\infty} \eta_{nm} P_n\left(\frac{c+d-z}{w}\right) e^{im\theta}. \tag{10}$$

Here $P_n(t)$ is the nth Legendre polynomial, $2w$ is the length of the region on each mirror illuminated by the beam, and $z = d$ and $z = c + d$ are the axial midpoints of the mirrors. The polynomial arguments $t = (d - z)/w$ and $t = (c + d - z)/w$ run from -1 to $+1$ as z runs over the illuminated parts of the mirrors. The first few Fourier-Legendre shapes are plotted in Figure 2. The relationship between the beam displacement $\delta(\theta)$ and the mirror error coefficients ψ_{nm} and η_{nm} can be found by substituting (10) into (2) and (3), and averaging the results over all the rays passing through the aperture. For a paraboloid alone this gives

$$\delta = \sum_{m=-\infty}^{\infty} \left[2(m-1)\Psi_{0m} + \frac{4l}{w}\Psi_{1m}\right] e^{i(m+1)\theta}, \tag{11}$$

and for a paraboloid and hyperboloid together

$$\delta = \sum_{m=-\infty}^{\infty} \left[(m+1)\Psi_{0m} - \frac{4a}{w}\Psi_{1m} + (m-3)\mathrm{H}_{0m} + \frac{4a}{w}\mathrm{H}_{1m}\right] e^{i(m+1)\theta}, \tag{12}$$

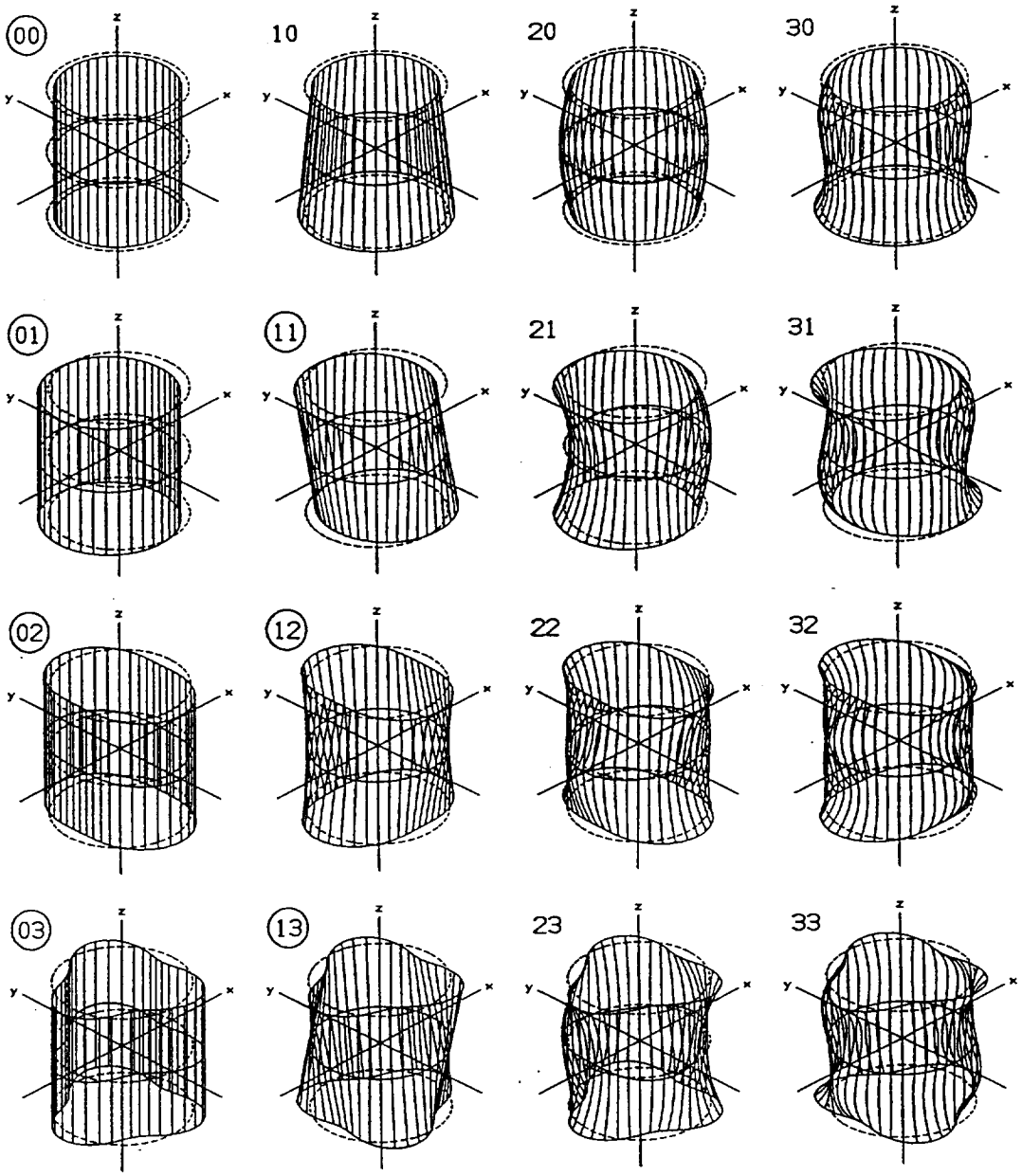

Figure 2: Fourier-Legendre mirror deformation terms for $nm = 00$ to 33 (n is order in z and m is order in θ). Alignment test can recognize only the circled terms; others will be aliased as one of the circled terms in the same row.

where Ψ_{0m}, Ψ_{1m}, H_{0m}, and H_{1m} are defined by

$$\begin{aligned} \Psi_{0m} &= \psi_{0m} - \tfrac{1}{8}\psi_{2m} - \tfrac{1}{64}\psi_{4m} - \cdots, \quad \Psi_{1m} = \psi_{1m} + \tfrac{3}{8}\psi_{3m} + \tfrac{15}{64}\psi_{5m} + \cdots, \\ \mathrm{H}_{0m} &= \eta_{0m} - \tfrac{1}{8}\eta_{2m} - \tfrac{1}{64}\eta_{4m} - \cdots, \quad \mathrm{H}_{1m} = \eta_{1m} + \tfrac{3}{8}\eta_{3m} + \tfrac{15}{64}\eta_{5m} + \cdots. \end{aligned} \tag{13}$$

These results were derived assuming the amplitude of the beam is uniform over the aperture. In practice the amplitude is actually Gaussian. The only effect that this will have is that in (13) the numerical coefficients multiplying ψ_{nm} and η_{nm} for $n \geq 2$ will be different.[1] If we equate the coefficients in series (11) and (7), we can solve for Ψ_{0m} and Ψ_{1m}:

$$\Psi_{0m} = \frac{1}{4m}\left(q_{1+m} - q_{1-m}^*\right), \quad \Psi_{1m} = \frac{w}{2l}\frac{1}{4m}\left[(1+m)q_{1+m} - (1-m)q_{1-m}^*\right], \tag{14}$$

where * denotes the complex conjugate. These results are not valid for $m = 0$; in that case we get only one equation: $\Psi_{00} - (2l/w)\Psi_{10} = -\frac{1}{2}q_1$. Thus the nonaxisymmetric components of the mirror shape error can be separated into even and odd components in z, but the axisymmetric components cannot. Similarly, for a paraboloid and hyperboloid together we get

$$\mathrm{H}_{0m} = \frac{1}{2m}\left(q_{1+m} - q_{1-m}^*\right) - \Psi_{0m}, \quad \mathrm{H}_{1m} = \frac{w}{4a}\frac{1}{2m}\left[(3+m)q_{1+m} - (3-m)q_{1-m}^*\right] + \Psi_{1m} - \frac{w}{a}\Psi_{0m}. \tag{15}$$

In this case when $m = 0$ we get $\mathrm{H}_{00} - (4a/3w)\mathrm{H}_{10} = -\frac{1}{3}q_1 + \frac{1}{3}[\Psi_{00} - (2l/w)\Psi_{10}]$. Note that in order to find the Fourier-Legendre coefficients for the hyperboloid it is necessary to have previously calculated those for the paraboloid. In general all of the Fourier-Legendre components shown in Figure 2 may be present in the mirror, but the alignment test system will "see" only the circled ones $nm = 00, 01, 11, 02, 12, 03, 13, \ldots$. For $m > 0$ the even terms $2m$, $4m$, ... are aliased as term $0m$, and the odd terms $3m$, $5m$, ... are aliased as term $1m$. For $m = 0$ all the terms are aliased as term 00. In practice, because the factors l/w and a/w in (11) and (12) are relatively large, the odd terms Ψ_{1m} and H_{1m} will tend to dominate the beam displacements.

Since we cannot actually calculate coefficients q_m, but only $\hat{q}_m$, we cannot actually calculate Ψ_{nm} and H_{nm}, but only $\hat{\Psi}_{nm}$ and $\hat{\mathrm{H}}_{nm}$, which will contain terms aliased in θ as well as z. The total number of coefficients that can be calculated for each n is N, the number of θ values at which measurements are taken. In particular, if N is even, we can calculate $\hat{\Psi}_{0m}$ and $\hat{\Psi}_{1m}$ for $m = 1$ to $N/2 - 1$, and some linear combination of $\hat{\Psi}_{0m}$ and $\hat{\Psi}_{1m}$ for $m = 0$ and $N/2$. We do not get two independent coefficients $\hat{\Psi}_{0m}$ and $\hat{\Psi}_{1m}$ for $m = N/2$ because $\hat{q}_{1+N/2}$ and $\hat{q}_{1-N/2}$ are not independent, but are related by equation (9).

3 ACF ERRORS

Equations (2) and (3) show that beam displacements caused by the ACF have the form

$$\delta(r,\theta) = \pm 2L\left(\frac{\partial f}{\partial x} \mp i\frac{\partial f}{\partial y}\right)e^{i(\theta \pm \theta)}. \tag{16}$$

In this equation, and everywhere else in this paper where $\pm$ or $\mp$ signs appear, the upper sign refers to the case of a paraboloid alone and the lower sign refers to the case of a paraboloid and hyperboloid together. The constant L in (16) is the focal length of the system, which is $L = l \approx 2a$ for a paraboloid alone and $L = a$ for a paraboloid and hyperboloid together. If we write $f(x,y)$ in the form

$$f(x,y) = \sum_{k=-\infty}^{\infty} C_k(r)e^{ik\theta}, \tag{17}$$

where the C_k's are unknown functions, then the total beam displacement will be

$$\delta(r,\theta) = \sum_{k=-\infty}^{\infty}\left[q_{k+1} \pm 2LD_k(r)\right]e^{i(k+1)\theta}, \quad \text{where} \quad D_k(r) = C_k'(r) \pm \frac{k}{r}C_k(r). \tag{18}$$

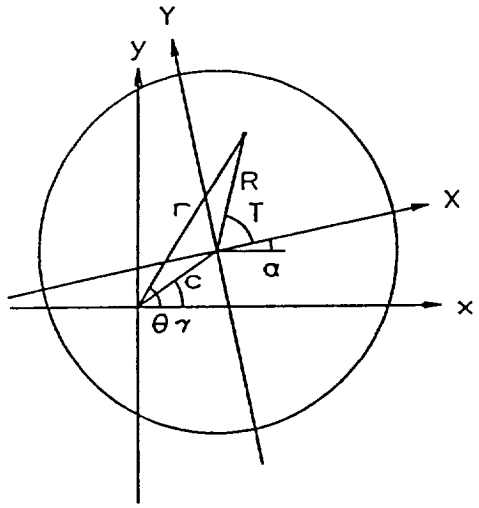

Figure 3: ACF moved to decentered position $ce^{i\gamma}$ and clocking angle α, as viewed from above.

The coefficients q_k represent the desired HRMA information, and the coefficients $2LD_k(r)$ represent the ACF errors. The Fourier coefficients ϕ_k calculated from these beam displacements using (6) will contain both the HRMA terms and the ACF terms: $\phi_k = \hat{q}_k \pm 2L\hat{D}_{k-1}(r)$. To obtain $\hat{q}_k$ from the calculated Fourier coefficient ϕ_k, we must know $2L\hat{D}_{k-1}(r)$.

Suppose that the ACF is translated in x and y by an amount $ce^{i\gamma}$ and rotated by an angle α, as shown in Figure 3, in which coordinate system XYZ is fixed in and moves with the ACF. We assume that the Z axis remains parallel to the z axis. (Section 5 discusses what happens if this is not the case.) It can be shown that the beam displacement with the ACF in this position will be

$$\delta(r,\theta,\gamma,\alpha) = \sum_{k=-\infty}^{\infty} \left[q_{k+1} \pm 2LE_k(r,\gamma,\alpha)\right] e^{i(k+1)\theta}, \tag{19}$$

where

$$E_k(r,\gamma,\alpha) = e^{-ik\alpha}\left[D_k(r) - \frac{c}{2}\left(e^{i(\gamma-\alpha)}D_{k+1}^{+}(r) + e^{-i(\gamma-\alpha)}D_{k-1}^{-}(r)\right)\right], \tag{20}$$

and where $D_k^{+}(r)$ and $D_k^{-}(r)$ are defined by

$$D_k^{+}(r) = D_k'(r) + \frac{k \mp 1}{r}D_k(r), \quad D_k^{-}(r) = D_k'(r) - \frac{k \mp 1}{r}D_k(r). \tag{21}$$

Equation (20) has been linearized with respect to the decentering distance c, so c must be small compared to the horizontal length scale of the variation in the ACF surface. By taking measurements for several values of γ and α it is possible to separate the error terms $E_k(r,\gamma,\alpha)$, which vary with γ and α, from the coefficients q_k, which do not.

Suppose that measurements are taken at beam positions $\theta_j = \theta_0 + 2\pi j/N$, $j = 0, 1, \ldots, N-1$, decentering angles $\gamma_j = 2\pi j/N_\gamma$, $j = 0, 1, \ldots, N_\gamma - 1$ (all at the same decentering distance c), and clocking angles $\alpha_j = 2\pi j/N_\alpha$, $j = 0, 1, \ldots, N_\alpha - 1$. We assume that N_α divides evenly into N, so that the same points on the ACF always line up with the apertures. All the information from the measurements can be extracted by taking Fourier transforms

with respect to θ, γ, and α, in turn:

$$\phi_k(\gamma,\alpha) = \frac{1}{N}\sum_{j=0}^{N-1}\delta(r,\theta_j,\gamma,\alpha)e^{-ik\theta_j}, \qquad k=0,1,\ldots,N-1, \tag{22}$$

$$\phi_{kl}(\alpha) = \frac{1}{N_\gamma}\sum_{j=0}^{N_\gamma-1}\phi_k(\gamma_j,\alpha)e^{-il\gamma_j}, \qquad l=0,1,\ldots,N_\gamma-1, \tag{23}$$

$$\phi_{klm} = \frac{1}{N_\alpha}\sum_{j=0}^{N_\alpha-1}\phi_{kl}(\alpha_j)e^{-im\alpha_j}, \qquad m=0,1,\ldots,N_\alpha-1. \tag{24}$$

The aliasing relationships for ϕ_{klm} are $\phi_{k+N,l,m} = e^{-iN\theta_0}\phi_{k,l,m}$ and $\phi_{k,l+N_\gamma,m} = \phi_{k,l,m+N_\alpha} = \phi_{k,l,m}$. If we transform (19) according to (22)–(24), we find that the only nonzero coefficients ϕ_{klm} are

$$\phi_{k+1,0,0} = \hat{q}_{k+1}, \quad \phi_{k+1,0,-k} = \pm 2L\hat{D}_k(r), \quad \phi_{k+1,1,-k-1} = \mp cL\hat{D}^+_{k+1}(r), \quad \phi_{k+1,-1,-k+1} = \mp cL\hat{D}^-_{k-1}(r). \tag{25}$$

The first two equations give the desired coefficients $\hat{q}_{k+1}$ and $\hat{D}_k(r)$. Because of aliasing, however, these two equations may not always be distinct. In particular, if k is a multiple of N_α they collapse into the single equation $\phi_{k+1,0,0} = \hat{q}_{k+1} \pm 2L\hat{D}_k(r)$, which makes it impossible to distinguish $\hat{q}_{k+1}$ from $\hat{D}_k(r)$. This is because these two equations represent information from the clocking angles, and it is impossible to determine $\hat{D}_k(r)$ using only information from the clocking angles. Obviously, it is impossible to determine the axisymmetric error term $\hat{D}_0(r)$ by simply rotating the ACF. Error terms of orders that are multiples of N_α appear axisymmetric when sampled at N_α points, and therefore cannot be determined either.

In these cases it is possible to calculate $\hat{D}_k(r)$ from the decentering terms $\hat{D}^+_k(r)$ and $\hat{D}^-_k(r)$. In particular, equation (21) gives

$$D_k(r) = \frac{r}{2(k\mp 1)}\left[D^+_k(r) - D^-_k(r)\right]. \tag{26}$$

Unfortunately, we are not dealing with $D_k(r)$, but with $\hat{D}_k(r)$, which includes aliased terms. Summing over the aliased terms, as in (8), gives

$$\hat{D}_k(r) = \frac{r}{2(k\mp 1)}\left[\hat{D}^+_k(r) - \hat{D}^-_k(r)\right] - \sum_{j=-\infty}^{\infty}\frac{jN}{k\mp 1}D_{k+jN}(r)e^{ijN\theta_0}. \tag{27}$$

We can approximate $\hat{D}_k(r)$ by the first term on the right hand side if the terms in the infinite sum are negligible. If the surface of the ACF is reasonably smooth, then the higher order terms should be small. We should therefore expect good results for small values of k, and in particular for $k=0$, which is the case of most interest. How many additional coefficients $\hat{D}_k(r)$ can be accurately determined in this way depends on the relative magnitudes of the higher order terms. In any case the approximation must break down by the time we reach $k=N/2$, since at that point the term $D_{-N/2}(r)$, which can be expected to be of the same order of magnitude as $D_{N/2}(r)$, appears as one of the error terms for $D_{N/2}(r)$.

It is also possible for other equations in (25) to be confounded by aliasing. This can be avoided by taking $N_\gamma \geq 3$ and $N_\alpha \geq 2$, or $N_\gamma \geq 2$ and $N_\alpha \geq 3$, either of which will insure that all the desired coefficients are distinct (except when k is a multiple of N_α, as described above). Partial results can be obtained using fewer tests. If $N_\gamma = 1$ (in which case $c=0$), or if $N_\gamma = 2$ and $N_\alpha \leq 2$, then the decentering information is lost, and it is possible to calculate only those coefficients $\hat{D}_k(r)$ and $\hat{q}_{k+1}$ for which k is not a multiple of N_α (which means it is impossible to calculate any coefficients if $N_\alpha = 1$). If $N_\gamma \geq 3$ and $N_\alpha = 1$, then the clocking information is lost; even so, it is still possible to calculate all coefficients except those for $k=1$ (for a paraboloid alone) or $k=-1$ (for a paraboloid and hyperboloid).

The ACF calibration process is summarized as follows. To do a full calibration test, we take beam displacement measurements $\delta(r,\theta,\gamma,\alpha)$ at N beam positions, N_γ decentering angles, and N_α clocking angles, where $N_\alpha \geq 2$

and $N_\gamma \geq 3$ or vice-versa, and where N_α divides evenly into N. We then calculate the Fourier coefficients ϕ_{klm} using (22)–(24). The calibration coefficients $\hat{D}_k(r)$ and misalignment coefficients $\hat{q}_k$ are then given by

$$2L\hat{D}_k(r) = \pm\phi_{k+1,0,-k} \quad \text{and} \quad \hat{q}_{k+1} = \phi_{k+1,0,0}, \tag{28}$$

unless k is zero or any other multiple of N_α, in which case we use

$$2L\hat{D}_k(r) = \mp\frac{r/c}{k \mp 1}(\phi_{k,1,0} - \phi_{k+2,-1,0}) \quad \text{and} \quad \hat{q}_{k+1} = \phi_{k+1,0,0} \mp 2L\hat{D}_k(r). \tag{29}$$

Calculating the calibration coefficients from clocking angle data using (28) is generally more accurate than calculating them from decentering data using (29). This is because rotating the ACF causes certain components of the ACF error to cancel exactly. In particular, rotating the ACF to N_α positions causes all Fourier components except multiples of N_α to cancel exactly. This enables (28) to give essentially perfect results when k is not a multiple of N_α. We have no choice but to calculate $\hat{D}_0(r)$ and $\hat{q}_1$ using decentering data, but the number of additional coefficients that must be calculated this way can be reduced by increasing the number of clocking angles.

Once calculated, the calibration coefficients $2L\hat{D}_k(r)$ can be used to perform further alignment tests with the ACF back in its home position ($c = 0$ and $\alpha = 0$). For each of these tests we take one set of beam displacement measurements $\delta(r,\theta)$ at N beam positions and calculate the Fourier coefficients ϕ_k using (6). The corrected misalignment coefficients are then given by $\hat{q}_{k+1} = \phi_{k+1} \mp 2L\hat{D}_k(r)$.

4 NUMERICAL SIMULATION

Some numerical simulations were performed to test the ACF calibration procedure and to estimate a suitable value for the decentering distance c. The results here are from a simulated calibration test using 384 beam displacements calculated at 24 beam positions, 4 decentering angles, and 4 clocking angles. The beam displacements were calculated using (16), and the calibration coefficients $\hat{D}_k(r)$ and misalignment coefficients $\hat{q}_k$ were calculated from the beam displacements as described in Section 3. The function $f(x,y)$ in (16) was taken to be a 16th-order Zernike polynomial fit of actual ACF surface data. The Zernike fit smooths some of the test noise and gives a differentiable function to use to calculate the beam displacements (16). We would expect the actual surface to be at least as smooth as the 16th order Zernike fit, but if this is not the case the actual errors may be larger than predicted here.

Figure 4 shows the real and imaginary components of the calculated hyperboloid calibration terms $2L\hat{D}_0(r)$ as a function of distance c for each of the six original mirror pairs $r = 607$, 547, 488, 431, 375, and 321 mm. Of the three calibration coefficients required for alignment purposes, $\hat{D}_0(r)$ will generally be the one with the highest error, since, unlike $\hat{D}_{-1}(r)$ and $\hat{D}_1(r)$, it is calculated from decentering data. It can be seen that the calculated values of $\hat{D}_0(r)$ are quite consistent for values of c up to about 10 or 20 mm, at which point they start to curve up or down. This suggests that c should not be larger than about 10 or 20 mm. The worst case, represented by solid lines, is for the outermost mirror pair at $r = 607$ mm, which lies fairly close to the outer edge of the ACF.

Figure 5 shows the error in coefficient $\hat{q}_1$, which, since it is corrected by $\hat{D}_0(r)$, will generally have the highest error. The solid line again represents the worst case $r = 607$ mm. For $c = 10$ mm the error is less than 1 μm for all r. The error curves are approximately straight lines with slope two, which indicates that the error is of order c^2. This is consistent with the derivation of the calibration procedure, in which only terms linear in c were kept. The fact that the errors are nicely proportional to c^2 implies that it should be possible to extend the calibration procedure to include the c^2 terms. This would make the analysis much more complicated, however, and would require taking measurements at more than one decentering distance c.

The errors in coefficients $\hat{q}_0$ and $\hat{q}_2$ for the simulated calibration test are essentially zero, because the corresponding ACF calibration coefficients $\hat{D}_{-1}(r)$ and $\hat{D}_1(r)$ can be determined essentially perfectly from the clocking

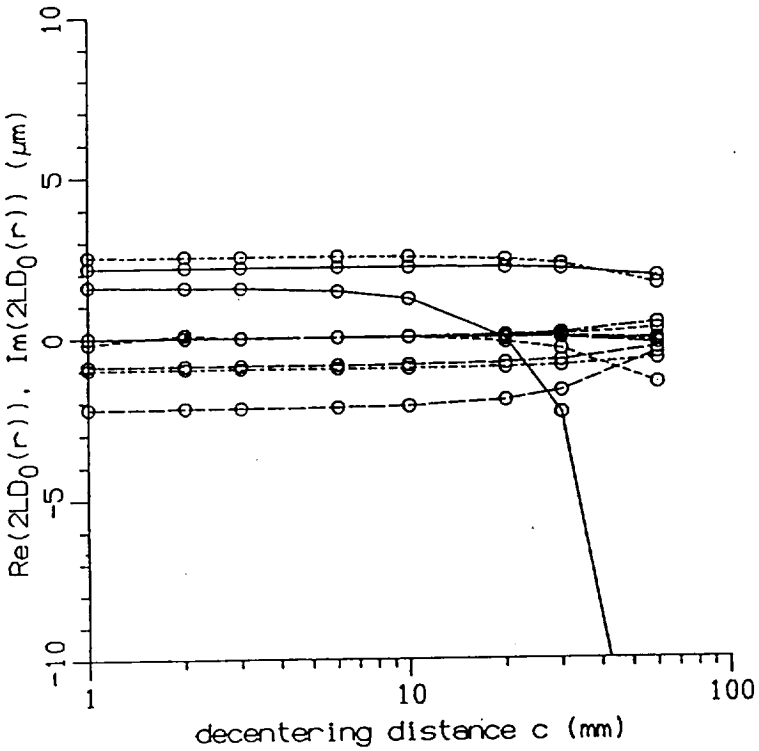

Figure 4: Calibration coefficient $\hat{D}_0(r)$ from simulated calibration test.

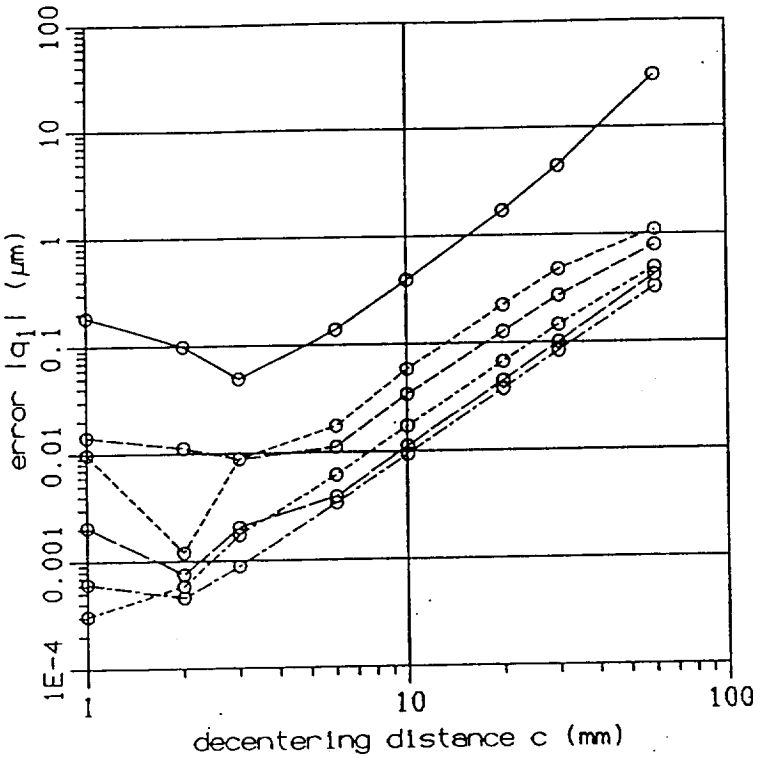

Figure 5: Error in coefficient $\hat{q}_1$ from simulated calibration test.

angle data. In this example we use four clocking angles, which gives essentially perfect results for all the coefficients except $\hat{D}_0(r)$, $\hat{D}_4(r)$, ..., $\hat{D}_{20}(r)$, and $\hat{q}_1$, $\hat{q}_5$, ..., $\hat{q}_{21}$.

5 ACF TILT

In the preceding section it was assumed that the ACF is not tilted when it is moved. This section discusses what will happen if this is not the case, and small random tilts occur. The resulting errors need not affect the alignment of the HRMA mirrors with respect to each other, but can affect the alignment of the HRMA as a whole with respect to an outside reference.

If the ACF is tilted, the function $f(x,y)$ specifying its surface will become $f(x,y) \to f(x,y) + Ax + By$, where A and B are constants. If the tilt changes each time the ACF is moved, A and B will be different for each ACF position. According to (16), the beam displacement will therefore become

$$\delta(r,\theta,\gamma,\alpha) \to \delta(r,\theta,\gamma,\alpha) \pm 2L\,[A(\gamma,\alpha) \mp iB(\gamma,\alpha)]\,e^{i(\theta\pm\theta)}, \tag{30}$$

where γ and α are the angles that determine the position of the ACF. If we define $C(\gamma,\alpha) = A(\gamma,\alpha) + iB(\gamma,\alpha)$, and substitute (30) into the Fourier transforms (22)–(24), we get

$$\begin{aligned} \phi_2(\gamma,\alpha) &\to \phi_2(\gamma,\alpha) + 2LC(\gamma,\alpha)^*, & \phi_0(\gamma,\alpha) &\to \phi_0(\gamma,\alpha) - 2LC(\gamma,\alpha), \\ \phi_{2l}(\alpha) &\to \phi_{2l}(\alpha) + 2LC_l(\alpha)^*, & \phi_{0l}(\alpha) &\to \phi_{0l}(\alpha) - 2LC_l(\alpha), \\ \phi_{2lm} &\to \phi_{2lm} + 2LC^*_{lm}, & \phi_{0lm} &\to \phi_{0lm} - 2LC_{lm}, \end{aligned} \tag{31}$$

where $C_l(\alpha) = A_l(\alpha) + iB_l(\alpha)$ is the Fourier transform of $C(\gamma,\alpha)$ with respect to γ, and $C_{lm} = A_{lm} + iB_{lm}$ is the Fourier transform of $C_l(\alpha)$ with respect to α. The results on the left are for a paraboloid, for which only coefficients with $k = 2$ are affected, and the results on the right are for a hyperboloid, for which only coefficients with $k = 0$ are affected. It follows that the results of a calibration test will change as follows:

$$\begin{aligned} 2LD_{-1}(r) &\to 2LD_{-1}(r) & 2LD_{-1}(r) &\to 2LD_{-1}(r) + 2LC_{01} \\ 2LD_0(r) &\to 2LD_0(r) - 2L(r/c)C^*_{-1,0} & 2LD_0(r) &\to 2LD_0(r) - 2L(r/c)C_{10} \\ 2LD_1(r) &\to 2LD_1(r) + 2LC^*_{0,-1} & 2LD_1(r) &\to 2LD_1(r) \\ q_0 &\to q_0 & q_0 &\to q_0 - 2LC_{00} \\ q_1 &\to q_1 + 2L(r/c)C^*_{-1,0} & q_1 &\to q_1 - 2L(r/c)C_{10} \\ q_2 &\to q_2 + 2LC^*_{00} & q_2 &\to q_2 \\ x_p + iy_p &\to x_p + iy_p & x_h + iy_h &\to x_h + iy_h - LC_{00} \\ z_p &\to z_p + (L^2/c)C^*_{-1,0} & z_h &\to z_h - (4L^2/5c)C_{10} \\ \alpha_p e^{i\beta_p} &\to \alpha_p e^{i\beta_p} - C_{00} & \alpha_h e^{i\beta_h} &\to \alpha_h e^{i\beta_h} - C_{00} \end{aligned} \tag{32}$$

The results on the left are for a paraboloid and the results on the right are for a hyperboloid. To estimate the magnitudes of the errors that will be produced in the calculated displacement and tilt of the HRMA we must make some assumptions about the possible values of the ACF tilts. If the slopes A and B are randomly distributed with mean zero and variance ϵ^2, that is, $E(A) = E(B) = 0$ and $E(A^2) = E(B^2) = \epsilon^2$, where $E(X)$ denotes the expected value of X, then $E(|C|^2) = 2\epsilon^2$. It can further be shown that $E(|C_{lm}|^2) = 2\epsilon^2/(N_\alpha N_\gamma)$ for any l and m. It follows that the expected errors in a calibration test are

$$\begin{aligned} E(x_p^2 + y_p^2)^{1/2} &= 0 &&= 0 & E(x_h^2 + y_h^2)^{1/2} &= L\sqrt{2}\epsilon_1 &&= 2.969\,\mu\text{m} \\ E(z_p^2)^{1/2} &= (L^2/c)\epsilon_1 &&= 8.397\,\text{mm} & E(z_h^2)^{1/2} &= (4L^2/5c)\epsilon_1 &&= 1.679\,\text{mm} \\ E(\alpha_p^2)^{1/2} &= \sqrt{2}\epsilon_1 &&= 0.061\,\text{arc sec} & E(\alpha_h^2)^{1/2} &= \sqrt{2}\epsilon_1 &&= 0.061\,\text{arc sec} \end{aligned} \tag{33}$$

where $\epsilon_1 = \epsilon/\sqrt{N_\alpha N_\gamma}$. The factor $\sqrt{2}$ is missing from the results for z_p and z_h because they are real rather than complex, so the imaginary part of the error can be ignored. The numerical values in (33) are for the specific case $N_\alpha = N_\gamma = 4$, $c = 10\,\text{mm}$, $L = 20\,\text{m}$ for a paraboloid and 10 m for a hyperboloid, and $\epsilon = 0.173\,\text{arc sec}$, which corresponds to A and B being uniformly distributed between $\pm 0.3\,\text{arc sec}$.

The errors resulting from ACF tilt may not generally be negligible, but since the tilt is the same over the whole ACF surface, the errors will be exactly the same for all HRMA mirrors measured using the same sequence of ACF tilts. Therefore, if the previously-installed mirrors are remeasured whenever a new mirror is added, and if the new mirror is adjusted so that its displacement and tilt match the new measurements of the previous mirrors, then all the mirrors will be correctly aligned with respect to each other, even though the displacement and tilt of the HRMA as a whole will be unknown, and will appear to change every time a new set of measurements with different ACF tilts is taken.

6 ACKNOWLEDGEMENTS

I would like to thank Art Jensen, who devised the basic plan for the ACF calibration and began this analysis, and Mark Waldman and John Hannon for several helpful discussions.

7 REFERENCES

[1] Timothy S. Lewis, "AXAF HRMA Alignment Test Analysis," Kodak Technical Report 287272F (AXAF document number XKR93-1831CD), 7 December 1993.

[2] R. Zimmerman, "Specification for the Finishing of the AXAF Mirror Elements," TRW Report EQ7-002 Revision B, 15 March 1991.

[3] Paul Glenn, "A set of orthonormal surface descriptors for near-cylindrical optics," *Optical Engineering*, **23**, No. 4, 1984, 178–186.